ISBN: 978-3-95450-232-5 ISSN: 2673-7000 doi:10.18429/JACoW-NAPAC2022-TUPA86

SIMULATIONS OF NANOBLADE CATHODE EMISSIONS WITH IMAGE CHARGE TRAPPING FOR YIELD AND BRIGHTNESS ANALYSES*

J. I. Mann†, B. Wang, G. E. Lawler, J. B. Rosenzweig, UCLA, Los Angeles, CA 90024, USA
S. Karkare, Arizona State University, Tempe, AZ 85287, USA
J. K. Nangoi, T. Arias, Cornell University, Ithaca, NY 14850, USA

Abstract

Laser-induced field emission from nanostructures as a means to create high brightness electron beams has been a continually growing topic of study. Experiments using nanoblade emitters have achieved peak fields upwards of 40 GV/m according to semi-classical analyses, begging further theoretical investigation. A recent paper has provided analytical reductions of the common semi-infinite Jellium system for pulsed incident lasers. We utilize these results to further understand the physics underlying electron rescattering-type emissions. We numerically evaluate this analytical solution to efficiently produce spectra and yield curves. The effect of space-charge trapping at emission may be simply included by directly modifying these spectra. Additionally, we use a self-consistent 1-D time-dependent Schrödinger equation with an image charge potential to study the same system as a more exact, but computationally costly, approach. With these results we may finally investigate the mean transverse energy and beam brightness at the cathode in these extreme regimes.

INTRODUCTION

The ubiquitous field of nanostructured cathodes has seen applications in electron microscopes [1], ultra-fast (low energy) electron diffraction [2], and electron guns in general [3]. The most common structure, the nanotip, field emits on the scale of 10s of nm, yielding excellent emittances. However, the tip is limited in the peak enhanced surface field that may be achieved, with material breakdown occurring at fields on the order of 10 GV/m [4, 5]. The goal of increasing brightness may be progressed by a similar nanostructure. The nanoblade [6, 7], which is essentially an extruded nanotip, has superior thermomechanical properties to the nanotip while supplying sufficient field enhancement to be compatible with tabletop lasers. Surface fields likely exceed 40 GV/m where space-charge (image-charge) limited current dominates emission statistics [8]. Measured emission energies around 500 eV [9] imply the existence of enhanced surface fields up to 80 GV/m by semi-classical analyses [10].

In this paper we continue the investigations of Refs. [6, 7] to model strong laser field emission from gold coated nanoblades. We first provide an update on our progress of evaluating the results of Ref. [11] for finding spectra. We modify our analytical image-charge (IC) trapping model in Ref. [6] to allow us to find the IC-modified (IC-M) spectra for exponential and arbitrary spectral profiles. In our full treatment of the system via the 1-D time-dependent Schrödinger equation (TDSE) with density-functional potentials, we transition from our planar-cylindrical Hartree model [6] to a solely cylindrical vacuum charge model to address computational issues noted in Ref. [7]. Unless otherwise stated we use Hartree atomic units (a.u.).

EVALUATION OF REF. [11]

Here we have progressed slightly from our previous results in Ref. [7]. We accelerated our implementation by improving parallelization and utilization of fast Fourier transforms. The yield at low incident fields agrees with the multi-photon emission order, $J \propto I^4$. However, at high fields where we would normally expect a tapering of yield due to channel closing, we instead observe a significant uptick in yield followed by noisy behavior. The energies supported in the calculation exceed $10U_p$ even within this problematic region, so mitigation of this problem is still in progress.

IMAGE-CHARGE TRAPPING MODEL

By treating the nanoblade as a long cylinder we may make great simplifications when analyzing the IC-M emissions. We note that laser-field emission tends to create broadband emissions, with a high-intensity direct emission process which decays exponentially with respect to emission energy on the scale of about $0.7U_p$, and with a low-intensity rescattering plateau which extends out to about $10U_p$. By making the assumption that electrons spatially resolve themselves quickly we may correlate their energy with their relative positions from the blade, with lower energies shielding higher energies.

The total image line charge λ_I within the cathode is equal and opposite to the total emitted line charge λ_0. With the energy-position correlation there is an effective image charge observed for each energy shell,

$$\lambda_I(E) = -\int_E^\infty dE' \frac{d\lambda}{dE'} \tag{1}$$

with $\frac{d\lambda}{dE'}$ the emission spectrum without any IC in consideration. The electrostatic potential difference between the nanostructure surface and far-vacuum is then approximately

$$\phi_I(E) = -2\ln\frac{a}{R}\int_E^\infty dE' \frac{d\lambda}{dE'} \tag{2}$$

for effective charge length a much larger than the apex radius of curvature R. If this is not true, then the original

* This research was funded by the Center for Bright Beams, National Science Foundation Grant No. PHY-1549132.
† jomann@physics.ucla.edu

ISBN: 978-3-95450-232-5 ISSN: 2673-7000 doi:10.18429/JACoW-NAPAC2022-TUPA86

expression may be used: $\ln \frac{a}{R} \to \ln\left[\sqrt{1+\frac{1}{4}\left(\frac{a}{R}\right)^2}+\frac{1}{2}\frac{a}{R}\right]$. Due to the logarithm, the emission dynamics are weakly dependent on the effective length scale. With this added potential depth the final emission energy will be $\mathcal{E} = E + \phi_I(E)$. By the chain rule, the spectrum would then be,

$$\frac{d\lambda}{d\mathcal{E}}(\mathcal{E}) = \left[1 + 2\frac{d\lambda}{dE}(E)\ln\frac{a}{R}\right]^{-1}\frac{d\lambda}{dE}(E) \tag{3}$$

The local spectral broadening is marked by the divisor expression. The initial energy E as a function of IC-M energy $\mathcal{E}$ would need to be substituted in this equation. As $\mathcal{E}$ is a monotonic function of E this is straightforward numerically.

By assuming an exponential unperturbed spectrum of the form $\frac{d\lambda}{dE} = \frac{\lambda_0}{\sigma}e^{-E/\sigma}$, $\mathcal{E}$ is analytically invertible, resulting in the final spectrum,

$$\frac{d\lambda}{d\mathcal{E}}(\mathcal{E}) = \frac{\frac{d\lambda}{dE}\left(\mathcal{E}+\sigma W\left(2\frac{\lambda_0}{\sigma}\ln\frac{a}{R}e^{-\frac{\mathcal{E}}{\sigma}}\right)\right)}{1+2\frac{\lambda_0}{\sigma}\ln\frac{a}{R}\exp\left(-\frac{\mathcal{E}+\sigma W\left(2\frac{\lambda_0}{\sigma}\ln\frac{a}{R}e^{-\frac{\mathcal{E}}{\sigma}}\right)}{\sigma}\right)} \tag{4}$$

where W denotes the Lambert W function. The high-energy plateau may be ignored due to its low charge content. The total yield may be calculated by integrating over the original spectrum starting from the turning point $\phi_I(E)+E = 0$. For the exponential profile,

$$\lambda_E = \frac{\lambda_0}{\sigma}\int_{E_t}^{\infty} dE\; e^{-\frac{E}{\sigma}} = \lambda_0\;\exp\left[-W\left(2\frac{\lambda_0}{\sigma}\ln\frac{a}{R}\right)\right] \tag{5}$$

for the turning point energy $E_t = \sigma W\left(2\frac{\lambda_0}{\sigma}\ln\frac{a}{R}\right)$. In the limit of strong IC at high field,

$$\lambda_E \approx \sigma\frac{\ln\left(2\frac{\lambda_0}{\sigma}\ln\frac{a}{R}\right)}{2\ln\frac{a}{R}} \propto \sigma \propto I_\gamma \tag{6}$$

We have thereby shown that, for high-intensity emissions from nanoblades, we expect a linear relationship between the yield and the laser intensity. We have previously considered that, for a planar system with zero-energy emission, equating the ponderomotive force with the image force also yields the same linear relationship [8]. These approaches mark two extremes: spectrally broad (and correlated) emissions with no extraction force and monochromatic emissions with an extraction force. The turning point energy in our calculations approximates the ponderomotive potential, and so both analyses seem to be at play to some extent.

IMAGE-CHARGE TDSE SIMULATION

Our previous results [7] uncovered a fundamental issue with how the density-functional electrostatic potential is modeled within our TDSE code. We noted that significant charge was being lost on the inner simulation boundary, creating excessive restoring forces.

We mitigate this issue by only modeling the image charge of vacuum electrons. Charges that are emitted from the surface are treated cylindrically such that they may exactly shield their equivalent image charge for electrons farther in vacuum, reducing computational costs. The image charge is opposite to the total freed electron charge and is distributed on a line at the center of the cylinder that makes the blade apex. The transition between material and vacuum is smoothed by a function mimicking the vacuum penetration scale at the Fermi level, $1 - e^{-\sqrt{2W}x}$ for $x > 0$.

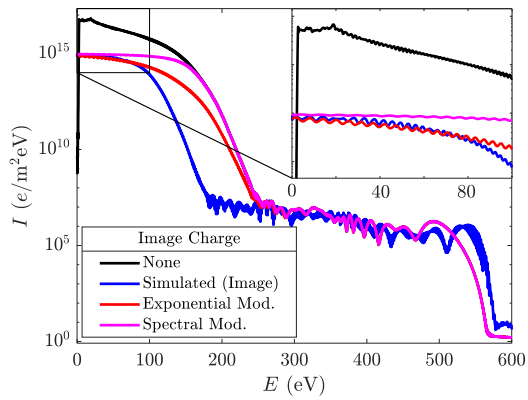

Figure 1: Spectra from laser field emission calculations with a peak field of 80 GV/m. The variations include a calculation without IC (black), the inclusion of IC within the TDSE (blue), the exponential-based modification (red), and the spectrum-based modification (magenta). The inset highlights the broadening and smearing of the $\hbar\omega$ peaks.

The results of this calculation and the application of the analytical image-charge trapping models are shown in Fig. 1. At 80 GV/m the non-IC spectrum is not quite exponential for $E < 25$ eV. Regardless, the exponential profile approximates the spectrum well as the image potential depth exceeds 25 eV. The simulated and analytical IC-M spectra all agree well using an illumination length of $a = 100$ µm and radius of curvature $R = 40$ nm. The TDSE IC calculation exhibits an energy suppression throughout the direct portion, indicating that there may be a collective potential that is overcome prior to the spatial resolving of the direct electrons.

The corresponding yield curves are in Fig. 2. Without the inclusion of IC the yield tapers off at high field strength due to channel closing. The mixed geometry Hartree model here and in Ref. [7] shows an inverse scaling at high field due to the excess charging problem. All three of the IC models qualitatively agree with each other and closely approach linear scaling at high laser intensities, resolving the excess charging issue. At low laser intensities the expected fourth-power scaling agrees with the multi-photon process order.

BRIGHTNESS ANALYSIS

We use the methods in Ref. [6] to calculate the intrinsic and surface curvature mean transverse energy (MTE). The MTEs are calculated using simulated data for a peak

ISBN: 978-3-95450-232-5 ISSN: 2673-7000 doi:10.18429/JACoW-NAPAC2022-TUPA86

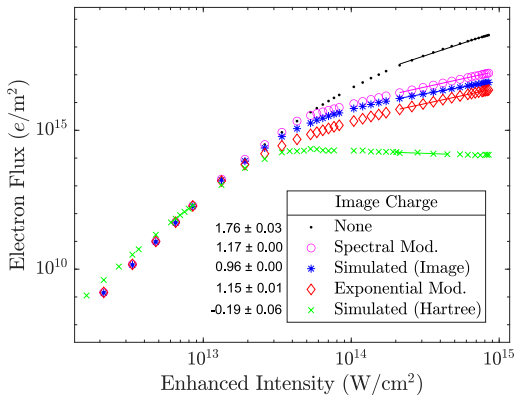

Figure 2: Yield curves for various IC models. Power law exponents fitted to the high-field data are shown next to their respective legend entries. Calculations include the TDSE with no IC (black dots), TDSE with IC only (blue asterisks), TDSE with mixed geometry [7] (green crosses), the spectrum-based IC model (magenta circles), and the exponential-based IC model (red diamonds).

surface field of 80 GV/m and a field profile $\cos\theta$, akin to a conducting cylinder in a uniform electric field. These MTE contributions, the total spectrum from the structure, and the RMS size of the beam are shown in Fig. 3. For a minimal emittance it is clear that one should filter the output such that only electrons near the direct cutoff (150 eV) or the rescattering cutoff (560 eV) are transmitted.

As for brightness, there is a local maximum near the rescattering cutoff at high energy and low charge. However, there is such a high current at very low energy that including all emissions nearly maximizes brightness. For comparably high current and low emittance, a window within the first MTE minimum around 150 eV may be ideal.

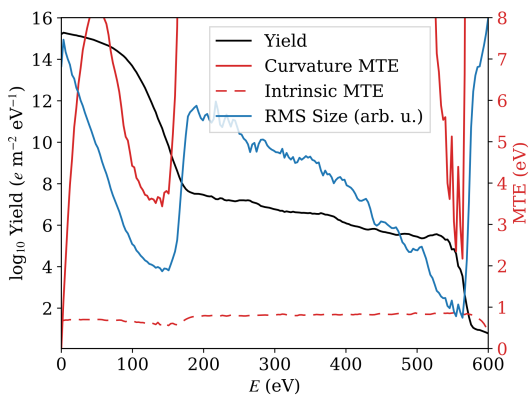

Figure 3: Total spectrum (black), the MTE due to blade curvature (red), the MTE due to the material's electronic distribution (dashed red), and the RMS size of the beam in the cross-blade direction (blue) for a peak field of 80 GV/m at the blade apex and with image charge included. The curvature MTE reaches a maximum of 54 eV in the plateau.

The transverse 2-D emittances are given by $\epsilon_2 = \sigma/\sqrt{\text{MTE}/mc^2}$. We denote the blade axis as the y-axis and the transverse axis perpendicular to y as the x-axis. The curvature and intrinsic MTE are added in quadrature for ϵ_x. The beam size in this axis is the angular RMS size times the radius, $\sigma_x = \sigma_\theta R$. Only the intrinsic MTE contributes to ϵ_y and the illumination length constitutes $\sigma_y = a$.

Table 1: Brightness and emittance for nanoblade emission at 80 GV/m, $a = 100\,\mu$m, and $R = 40$ nm. The high energy (High-E) samples are given by a Gaussian filter with spread and central energy set to optimize B_6. The Full-Spec samples do not filter the spectrum. IC indicates that Brithe calculation used image charge, and NC calculations did not.

Regime	B_6	B_5	ϵ_x	ϵ_y
	A/μm^{2}mrad^2		nm-mrad	
High-E (IC)	5.72E-8	2.41E-10	18.0	1.23E5
High-E (NC)	1.09E-9	4.94E-10	18.4	1.33E5
Full-Spec (IC)	146	0.984	60.0	1.17E5
Full-Spec (NC)	6630	47.0	45.2	1.27E5

The 4-D brightness for a yield of Q is $B_4 = \frac{Q}{\epsilon_x \epsilon_y}$. For the 5-D brightness we divide the yield by the full-width half-maximum power of the laser, $\tau = 8$ fs in our simulations, to get the pulse-averaged current. For the 6-D brightness we further divide by the normalized RMS normal energy spread, $\sqrt{\sigma_E/mc^2}$. These quantities are shown in Table 1. B_6 is optimized near the rescattering cutoff by applying a Gaussian window with a center and width of $E_0 = 535$ eV and $\sigma_E = 11.3$ eV. The full spectrum brightness is around 10 orders of magnitude larger than the high-energy optimized sample. This is because the plateau contains exponentially less current than the direct portion, while optimization only improves emittance by a factor of about 3.

We note that the full emission brightness increases with field strength due to the increase in current. The minimum emittance achievable at the rescattering cutoff increases with field strength as the curvature MTE is proportional to the ponderomotive energy [6]. In the unfiltered spectrum, IC decreases current and therefore decreases brightness by a significant amount. For an optimized high-energy window, IC only decreases brightness by about a factor of two.

CONCLUSION

We have shown that the yield from strong field emission from nanoblades is proportional to the laser intensity by a second method. This is corroborated by previous observations [8]. The fictitious loss of charge in Ref. [7] is resolved by switching to a solely image-charge model. The new image charge model for the TDSE predicts nearly linear high intensity behaviour as expected. The emission's brightness and emittances are also promising, with two use cases being high current from the entire spectrum or a low emittance with low current at high normal energy. Further investigation and measurement of these properties are in progress.

ISBN: 978-3-95450-232-5 ISSN: 2673-7000 doi:10.18429/JACoW-NAPAC2022-TUPA86

REFERENCES

[1] R. Bormann, S. Strauch, S. Schäfer, and C. Ropers, "An ultrafast electron microscope gun driven by two-photon photoemission from a nanotip cathode," *Journal of Applied Physics*, vol. 118, no. 17, p. 173 105, 2015. doi:10.1063/1.4934681

[2] G. Storeck, S. Vogelgesang, M. Sivis, S. Schäfer, and C. Ropers, "Nanotip-based photoelectron microgun for ultrafast leed," *Structural Dynamics*, vol. 4, no. 4, p. 044 024, 2017. doi:10.1063/1.4982947

[3] B. Schröder, M. Sivis, R. Bormann, S. Schäfer, and C. Ropers, "An ultrafast nanotip electron gun triggered by grating-coupled surface plasmons," *Applied Physics Letters*, vol. 107, no. 23, p. 231 105, 2015. doi:10.1063/1.4937121

[4] M. Krüger, C. Lemell, G. Wachter, J. Burgdörfer, and P. Hommelhoff, "Attosecond physics phenomena at nanometric tips," *Journal of Physics B: Atomic, Molecular and Optical Physics*, vol. 51, no. 17, p. 172 001, 2018. doi:10.1088/1361-6455/aac6ac

[5] R. Bormann, M. Gulde, A. Weismann, S. V. Yalunin, and C. Ropers, "Tip-enhanced strong-field photoemission," *Phys. Rev. Lett.*, vol. 105, p. 147 601, 14 2010. doi:10.1103/PhysRevLett.105.147601

[6] J. I. Mann, T. Arias, G. E. Lawler, J. K. Nangoi, and J. B. Rosenzweig, "Simulations of Nanoblade-Enhanced Laser-Induced Cathode Emissions and Analyses of Yield, MTE, and Brightness," in *Proc. IPAC'21*, Campinas, Brazil, May 2021, pp. 2957–2960. doi:10.18429/JACoW-IPAC2021-WEPAB147

[7] B. Wang *et al.*, "Simulations of Laser Field Emission from Nanostructures with Image Charge Trapping and Band Structure Transitions," in *Proc. IPAC'22*, Bangkok, Thailand, 2022, pp. 717–720. doi:10.18429/JACoW-IPAC2022-MOPOMS036

[8] T. Paschen *et al.*, "Near-field-driven electron rescattering at a nanoblade," unpublished.

[9] G. E. Lawler, N. Majernik, J. I. Mann, N. E. Montanez, J. B. Rosenzweig, and V. S. Yu, "Emittance Measurements of Nanoblade-Enhanced High Field Cathode," in *Proc. IPAC'22*, Bangkok, Thailand, 2022, pp. 709–712. doi:10.18429/JACoW-IPAC2022-MOPOMS033

[10] J. Mann and J. Rosenzweig, "Semi-classical cutoff energies for electron emission and scattering at field-enhancing nanostructures with large ponderomotive amplitudes," 2021. doi:10.48550/ARXIV.2105.10601

[11] Y. Luo, Y. Zhou, and P. Zhang, "Few-cycle optical-field-induced photoemission from biased surfaces: An exact quantum theory," *Phys. Rev. B*, vol. 103, p. 085 410, 8 2021. doi:10.1103/PhysRevB.103.085410